animals

MDPI

Article

Histological and Histopathological Features of the Third Metacarpal/Tarsal Parasagittal Groove and Proximal Phalanx Sagittal Groove in Thoroughbred Horses with Racing History

Szu-Ting Lin [1], Alastair K. Foote [2], Nicholas M. Bolas [3], David R. Sargan [1] and Rachel C. Murray [2,*]

[1] Department of Veterinary Medicine, University of Cambridge, Madingley Rd, Cambridge CB3 0ES, UK; linstjulie@outlook.com (S.-T.L.); drs20@cam.ac.uk (D.R.S.)
[2] Rossdales Veterinary Surgeons, Cotton End Rd, Exning, Newmarket CB8 7NN, UK; alastair.foote@rossdales.com
[3] Hallmarq Veterinary Imaging, Unit 5 Bridge Park, Merrow Lane, Guildford GU4 7BF, UK; nick.bolas@hallmarq.net
* Correspondence: rachel.murray@rossdales.com

Simple Summary: Information about the histological features of the proximal phalanx (P1) sagittal groove in racehorses is limited compared to the third metacarpal/metatarsal parasagittal groove. Fractures of the P1 sagittal groove are common in racehorses; therefore, it is important to improve the understanding of the histopathology of the P1 sagittal groove. This study aims to describe histopathological features of the third metacarpal/metatarsal parasagittal groove and the proximal phalanx sagittal groove in Thoroughbred racehorses. For third metacarpal/metatarsal parasagittal grooves, hyaline cartilage (HC), calcified cartilage (CC), and subchondral plate and trabecular bone (SCB/TB) histopathology including SCB collapse were most severe in locations with fissures (observed in a previous study) and the palmar/plantar aspect of the parasagittal groove. For P1 sagittal grooves, SCB/TB histopathology was most severe in locations with fissures, and SCB collapse was most severe in the dorsal and middle aspects of sagittal groove. In conclusion, histopathological features of bone fatigue injury were related to fissure locations, the palmar/plantar third metacarpal/metatarsal parasagittal groove, and the dorsal P1 sagittal groove. Histopathological findings in the P1 sagittal groove may be useful for investigating the pathogenesis of P1 sagittal groove fractures.

Abstract: Information regarding the histopathology of the proximal phalanx (P1) sagittal groove in racehorses is limited. Twenty-nine cadaver limbs from nine Thoroughbred racehorses in racing/race-training underwent histological examination. Histological specimens of the third metacarpal/metatarsal (MC3/MT3) parasagittal grooves and P1 sagittal grooves were graded for histopathological findings in hyaline cartilage (HC), calcified cartilage (CC), and subchondral plate and trabecular bone (SCB/TB) regions. Histopathological grades were compared between (1) fissure and non-fissure locations observed in a previous study and (2) dorsal, middle, and palmar/plantar aspects. (1) HC, CC, and SCB/TB grades were more severe in fissure than non-fissure locations in the MC3/MT3 parasagittal groove ($p < 0.001$). SCB/TB grades were more severe in fissure than non-fissure locations in the P1 sagittal groove ($p < 0.001$). (2) HC, CC, and SCB/TB grades including SCB collapse were more severe in the palmar/plantar than the middle aspect of the MC3/MT3 parasagittal groove ($p < 0.001$). SCB/TB grades including SCB collapse were more severe in the dorsal and middle than the palmar/plantar aspect of the P1 sagittal groove ($p < 0.001$). Histopathology in the SCB/TB region including bone fatigue injury was related to fissure locations, the palmar/plantar MC3/MT3 parasagittal groove, and the dorsal P1 sagittal groove.

Keywords: subchondral bone; articular cartilage; proximal phalanx sagittal groove; metacarpal/metatarsal parasagittal groove; fissure; thoroughbred

check for updates

Citation: Lin, S.-T.; Foote, A.K.; Bolas, N.M.; Sargan, D.R.; Murray, R.C. Histological and Histopathological Features of the Third Metacarpal/Tarsal Parasagittal Groove and Proximal Phalanx Sagittal Groove in Thoroughbred Horses with Racing History. *Animals* **2024**, *14*, 1942. https://doi.org/10.3390/ani14131942

Academic Editor: Drew W. Koch

Received: 23 May 2024
Revised: 23 June 2024
Accepted: 26 June 2024
Published: 30 June 2024

Copyright: © 2024 by the authors. Licensee MDPI, Basel, Switzerland. This article is an open access article distributed under the terms and conditions of the Creative Commons Attribution (CC BY) license (https://creativecommons.org/licenses/by/4.0/).

1. Introduction

Third metacarpal/metatarsal (MC3/MT3) parasagittal groove fracture (parasagittal fracture) and proximal phalanx (P1) sagittal groove fracture (sagittal fracture) are the most common fractures in Thoroughbred racehorses [1–4]. The risk factors [1,5–7], pathogenesis [8–11], and macroscopic findings [8–10,12–14] of parasagittal fractures have been well reported in previous studies. Parasagittal fractures in racehorses occur in predictable locations and are considered to be stress fractures [8–11,14,15]. It has been suggested that stress fracture occurs as subchondral bone adaptation fails [8–11,15]. Previous microscopic studies found that microcracks in the calcified cartilage and subchondral bone accumulated during repetitive bone injuries from high-speed exercises, and the coalescing and propagation of microcracks could be a predisposing factor in the development of stress fracture [8–11,15]. Pathological changes in linear defects in the calcified cartilage and subchondral bone (defined as fissures in this study) have also been observed in the MC3/MT3 parasagittal groove at locations where fractures originate [10,12,13,16]; therefore, it has been suggested that fissures could be one of the prodromal pathologies of stress fractures [9,10,12,13,16].

A sagittal fracture of P1 used to be considered as resulting from a single acute traumatic event, but imaging studies on racehorses and sport horses have shown that sagittal fractures may also develop from fatigue injuries [17–24]. Imaging studies suggested that the aetiology of sagittal fractures may be similar to parasagittal fractures, developing from failure of functional adaptation in subchondral bone and the propagation of microcracks into stress fractures [17–20]. Therefore, fissures were also suggested to be one of the prodromal pathologies of sagittal fractures [18]. Histological studies are needed to assess the relation between imaging findings of fissures and fatigue injuries [17]. However, there are no reports of histopathological findings in the proximal phalanx sagittal groove to the authors' knowledge, except for a microcomputed tomography study reporting the adaptation of subchondral bone to race training including increased subchondral bone thickness and volumetric bone mineral density [25].

The objectives of this study were to describe the histopathological features of the MC3/MT3 parasagittal groove and P1 sagittal groove in Thoroughbred racehorses using the following two approaches:

- A comparison between locations with and without fissures in the MC3/MT3 parasagittal groove and P1 sagittal groove detected in a previous study [26]. In the previous study, fissures were identified on both cone-beam and fan-beam computed tomography and were confirmed as histological findings of microcracks in the calcified cartilage and subchondral bone plate [26]. The previous study assessed histopathological features associated with fissures regardless of MC3/MT3 or P1 origin [26]. In this study, fissures of MC3/MT3 or P1 origin were described separately.
- A comparison between dorsal, middle, and palmar/plantar aspects of the MC3/MT3 parasagittal groove and P1 sagittal groove.

It was hypothesised that (1) the histopathological features of locations with fissures would be similar between the MC3/MT3 parasagittal groove and P1 sagittal groove and (2) predilection sites of parasagittal fractures and sagittal fractures including the palmar/plantar aspect of the MC3/MT3 parasagittal groove and the dorsal and middle aspects of the P1 sagittal groove would be more associated with histopathological features of stress/fatigue injuries.

2. Materials and Methods

2.1. Materials

The study was approved by the University of Cambridge Ethical Review committee (project number: CR558).

Twenty-nine cadaver limbs (fifteen forelimbs and fourteen hindlimbs) from 9 Thoroughbred horses (6 geldings, 2 colts, and 1 filly) aged 2–11 years were used in this study. The cadaver limbs were convenience samples from a previous study [26]. All horses had racing or race-training history. Limbs were sourced entirely from the UK where Thorough-

bred racehorses are trained and raced in both directions (clockwise and anticlockwise), with training taking place off the racecourse. All horses were euthanised for reasons other than the study: 5 due to fractures (P1 fractures, medial condylar fracture, lateral condylar fracture, and proximal sesamoid bone fracture in other limbs) and 4 for reasons other than fracture (severe osteoarthritis, severe osteochondral lesion, head injury, and pelvic injury). The cadaver limbs from horses with fractures were not entirely excluded from the study, but locations affected by complete fractures were excluded from histological examination. See Figure 1.

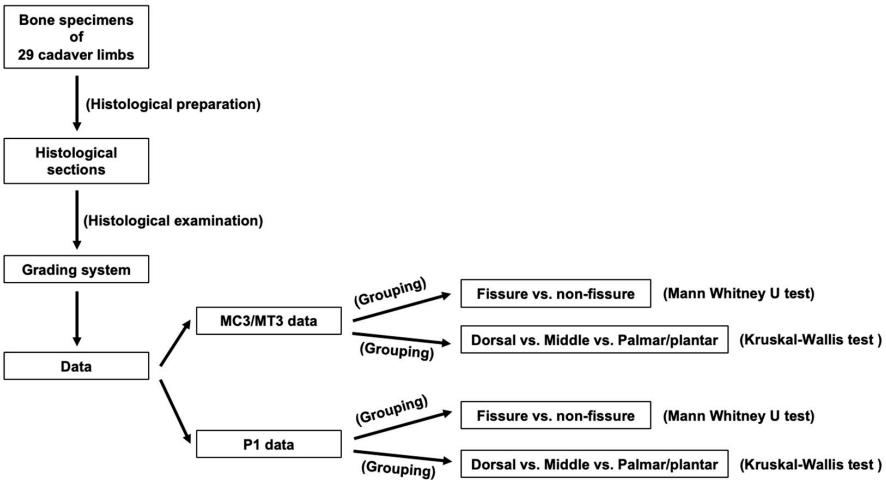


Figure 1. Schematic overview of the study including histological preparation, examination, grading, and data analysis. The grouping of fissures was defined in the previously published study, where fissures were identified on both cone-beam and fan-beam computed tomography and were confirmed by histological examination [26].

Cadaveric limbs were collected at the carpus or tarsus level within 8 h of euthanasia and stored frozen at −20 °C. The limbs were thawed at room temperature for 24 h before post-mortem examination.

2.2. Histological Preparation

For each cadaver limb, bone specimens (4–5 mm thickness) were collected using a band saw at the dorsal, middle, and palmar/plantar aspects of the MC3/MT3 parasagittal groove and P1 sagittal groove (Figures 2 and 3). Dorsal, middle, and palmar/plantar aspects were divided by the dorsal and palmar/plantar borders of the collateral fossae. Collected bone specimens were then fixed in 10% neutral buffered formalin for 7 days minimum, decalcified in hydrochloric acid for 2 days minimum, and paraffin embedded. Histological sections (4–5 µm thickness) were stained with haematoxylin and eosin (H&E) and toluidine blue.

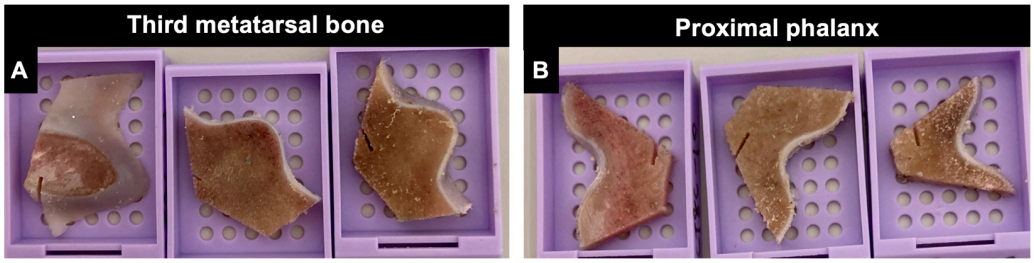


Figure 2. Bone specimens from a hindlimb. From left to right: bone specimens collected from the dorsal, middle, and plantar aspects of the third metatarsal parasagittal groove (**A**) and proximal phalanx sagittal groove (**B**). The lateral side of the specimen was marked using a bandsaw. The shape of specimens from the third metacarpal bone is different from specimens from the proximal phalanx.

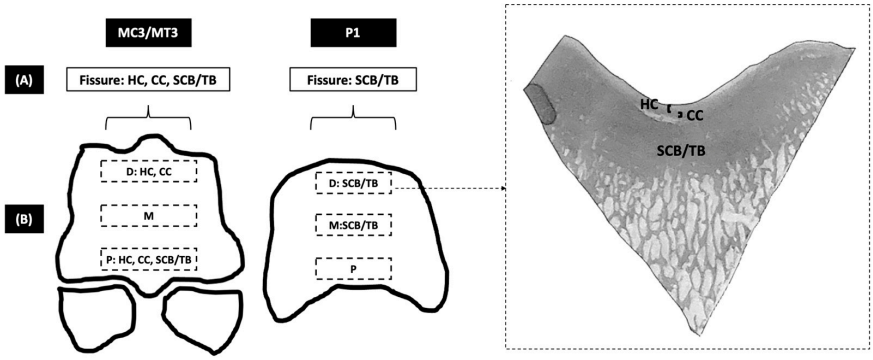


Figure 3. Illustration of the regions graded for histopathological changes, grouped for comparison, and outcome. Histological specimen in the box on the right demonstrated regions of hyaline cartilage (HC), calcified cartilage (CC), and subchondral plate and trabecular bone regions (SCB/TB). Histopathological grades from third metacarpal/metatarsal (MC3/MT3) and proximal phalanx (P1) were analysed separately and were compared using two approaches: (**A**) fissure and non-fissure locations and (**B**) dorsal (D), middle (M), and palmar/plantar (P) aspects. HC, CC, and SCB grades were most severe in fissure locations and the palmar/plantar aspect of the MC3/MT3 parasagittal groove. SCB grades were most severe in fissure locations and the dorsal and middle aspects of the P1 sagittal groove.

2.3. Histological Examination

Histological sections were graded for histopathological changes using a previously published grading system by a trained interpreter (PhD student) and overseen by recognised specialists (Alastair K. Foote and Rachel C. Murray) [27]. The interpreter was not aware of the location (dorsal, middle, and palmar/plantar) or the identity of the histological sections. However, fissures and the origin of sections from either a third metacarpal/metatarsal bone or a proximal phalanx could not be blinded due to the concurrent presence of fissures with histopathological changes and the shape of sections (Figure 2).

The grading of histopathological changes included the following three regions based on a previously published grading system [27] (Figure 3):

(1) Hyaline cartilage (HC): alteration in staining for glycosaminoglycans, surface irregularity, fibrillation, thickness variation, irregular chondrocyte distribution, chondrocyte loss, and chondrocyte clustering.
(2) Calcified cartilage (CC): tidemark incongruence, calcified cartilage cleft, depth variation, vascular invasion, and islands of cartilage in subchondral bone plate.
(3) Subchondral plate and trabecular bone regions (SCB/TB): sclerosis, subchondral bone collapse, the replacement of cancellous bone with dense bone, trabecular thickening, replacement with osteonal bone (increased deposition of lamellar bone), increased basic multicellular units (BMUs), replacement with woven bone, and Howship's lacunae.

For each region, histological grades ranged from 0 (no abnormality) to 3 (severe histopathology). Representative images of the grades of histopathological changes are provided in Supplementary Figures S1–S3.

2.4. Histological Grades Analysis

Histological grades established in the previous study were further analysed in this study [26]. Different from the previous study [26], histological grades from MC3/MT3 and P1 were analysed separately. The grading of each histopathologic specimen in the HC, CC, and SCB/TB regions and the summary (by pooling) of all grades in each region used the following two independent grouping approaches (Figure 3):

A. Grouping by the presence or absence of fissures observed in the previous study, where fissures were identified on both cone-beam and fan-beam computed tomography and

were confirmed by histological examination [26]: (1) fissure location and (2) non-fissure location.

B. Grouping by dorsal, middle, and palmar/plantar aspects, where bone specimens were collected (see Histological Preparation for details): (1) dorsal aspect, (2) middle aspect, and (3) palmar/plantar aspect.

2.5. Data Analysis

Statistical analyses were performed using IBM SPSS Statistics 28.0.0 software. The comparison of histological grades between fissure and non-fissure locations in the MC3/MT3 parasagittal groove and P1 sagittal groove was performed using the Mann–Whitney U test. The comparison of histological grades between the dorsal, middle, and palmar/plantar aspects of the MC3/MT3 parasagittal groove and P1 sagittal groove was performed using the Kruskal–Wallis test and a post hoc Mann–Whitney U test. A p value < 0.05 was considered statistically significant. Differences in histopathological features between the MC3/MT3 parasagittal groove and P1 sagittal groove were described.

3. Results

Of the 29 cadaver limbs in this study, 1had MC3 lateral parasagittal groove complete fracture, 1 had P1 sagittal groove complete fracture, 1 had P1 sagittal groove incomplete fracture, and the remaining 26 limbs were not affected by MC3/MT3/P1 fractures.

3.1. Comparison between Fissure and Non-Fissure Locations in MC3/MT3 and P1 (Figure 4)

See Table 1 and Figure 5 for details of the comparison of grades of each histopathological change in the HC, CC, and SCB/TB regions and the proportion of grades in fissure and non-fissure locations.

Table 1. Significance of differences in histopathological grades compared between fissure and non-fissure locations. MC3/MT3: third metacarpal/metatarsal parasagittal groove. P1: proximal phalanx sagittal groove. Numbers presented in the table are p values.

Items	MC3/MT3	P1
Hyaline cartilage		
Reduced staining for glycosaminoglycans in cartilage	0.001 *	0.70
Cartilage surface irregularity	<0.001 **	0.86
Cartilage fibrillation	0.25	0.86
Cartilage thickness variation	0.13	0.88
Irregular chondrocyte distribution	<0.001 **	0.50
Chondrocyte loss/necrosis	<0.001 **	0.15
Chondrocyte clustering	0.13	0.08
Summary of hyaline cartilage	<0.001 **	0.82
Calcified cartilage		
Tidemark incongruence	<0.001 **	0.36
Calcified cartilage cleft	0.003 *	1.0
Calcified cartilage depth variation	<0.001 **	0.71
Vascular invasion	<0.001 **	<0.001 **
Islands of hyaline cartilage in subchondral bone plate	0.07	0.38
Summary of calcified cartilage	<0.001 **	0.17
Subchondral plate and trabecular bone		
Sclerosis of subchondral bone plate and adjacent cancellous bone	<0.001 **	0.004 *
Subchondral bone collapse	<0.001 **	0.24
Replacement of cancellous bone with dense bone	<0.001 **	<0.001 **
Trabecular thickening with reduced marrow spaces	<0.001 **	<0.001 **
Replacement with osteonal/lamellar bone	<0.001 **	<0.001 **
Increased basic multicellular units	<0.001 **	0.02 *
Replacement with woven bone	<0.001 **	0.83
Howship's lacunae with/without osteoclast	0.40	0.77
Summary of subchondral plate and trabecular bone	<0.001 **	<0.001 **

* Significant difference (fissure > non-fissure location). ** Highly significant difference (fissure > non-fissure location).

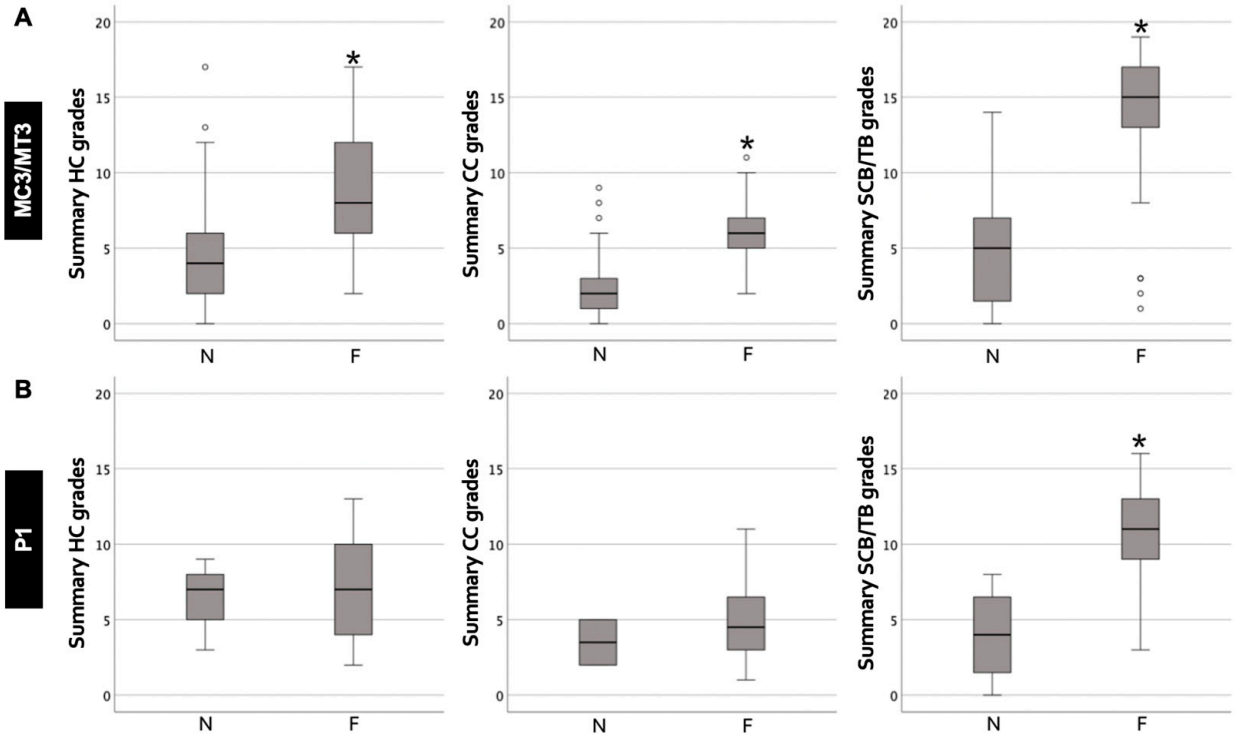


Figure 4. Summary of histological grades compared between fissure and non-fissure locations. HC (hyaline cartilage); CC (calcified cartilage); SCB/TB (subchondral plate and trabecular bone). (**A**) HC, CC, and SCB/TB histological grades were more severe in fissure (F) than non-fissure (N) locations in the third metacarpal/tarsal parasagittal groove (MC3/MT3). (**B**) SCB/TB histological grades were more severe in F than N locations in the proximal phalanx sagittal groove (P1). * Significant difference ($p < 0.001$). Circles above or below the end of the whiskers represented outliers.

3.1.1. MC3/MT3 Parasagittal Groove

The median value and interquartile range of summary of histological grades for (1) fissure locations were 8.0 ± 7.0 in the HC region ($n = 41$), 6.0 ± 2.0 in the CC region ($n = 41$), and 15.0 ± 5.0 in the SCB/TB region ($n = 45$); and (2) non-fissure locations were 4.0 ± 5.0 in the HC region ($n = 61$), 2.0 ± 2.0 in the CC region ($n = 59$), and 5.0 ± 6.0 in the SCB/TB region ($n = 67$). The summary of the HC, CC, and SCB/TB histological grades was more severe in the fissure than non-fissure locations ($p < 0.001$ for all comparisons; Figure 3).

3.1.2. P1 Sagittal Groove

The median value and interquartile range of the summary of histological grades for (1) fissure locations were 7.0 ± 6.0 in the HC region ($n = 41$), 4.5 ± 4.0 in the CC region ($n = 40$), and 11.0 ± 4.0 in the SCB/TB region ($n = 42$); and (2) non-fissure locations were 7.0 ± 4.0 in the HC region ($n = 6$), 3.5 ± 3.0 in the CC region ($n = 6$), and 4.0 ± 7.0 in the SCB/TB region ($n = 7$). The summary of the SCB/TB histological grades was more severe in fissure than non-fissure locations ($p < 0.001$), while there was no significant difference in the summaries of the HC and CC histological grades (Figure 3).

3.2. Comparison between Dorsal, Middle, and Palmar/Plantar Aspects in MC3/MT3 and P1 (Figure 6)

See Table 2 and Figure 7 for details of the comparison of grades of each histopathological change in the HC, CC, and SCB/TB regions and the proportion of grades in the dorsal, middle, and palmar/plantar aspects.

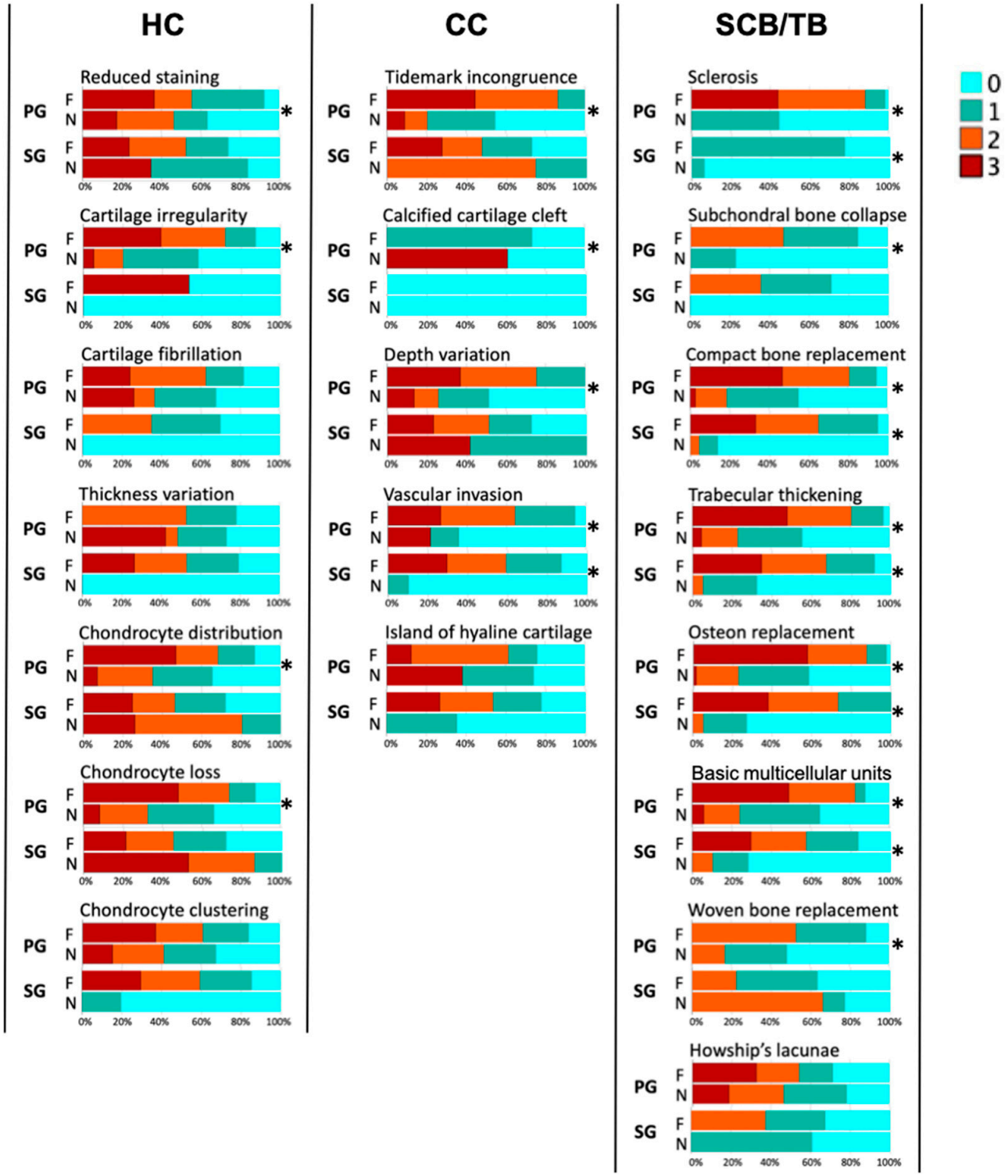


Figure 5. Proportion of grades for fissure and non-fissure locations. HC (hyaline cartilage); CC (calcified cartilage); SCB/TB (subchondral plate and trabecular bone); PG (third metacarpal/metatarsal parasagittal groove); SG (proximal phalanx sagittal groove); F (fissure location); N (non-fissure location). * Significant difference ($p < 0.05$).

Table 2. Significance of differences in histopathological grades compared between dorsal, middle, and palmar/plantar aspects. MC3/MT3: third metacarpal/metatarsal parasagittal groove. P1: proximal phalanx sagittal groove. D: dorsal. M: middle. P: palmar/plantar. Numbers presented in the table are *p* values.

Items	MC3/MT3	Post Hoc	P1	Post Hoc
Hyaline cartilage				
Reduced staining for glycosaminoglycans in cartilage	<0.001 **	D > M P > M	0.36	-
Cartilage surface irregularity	<0.001 **	D > M P > M	0.14	-
Cartilage fibrillation	<0.001 **	D > M D > P	0.14	-
Cartilage thickness variation	<0.001 **	D > M P > M	0.07	-
Irregular chondrocyte distribution	<0.001 **	D > M P > M	0.62	-
Chondrocyte loss/necrosis	<0.001 **	D > M P > M	0.15	-
Chondrocyte clustering	0.10	-	0.90	-
Summary of hyaline cartilage	<0.001 **	D > M P > M	0.70	-
Calcified cartilage				
Tidemark incongruence	<0.001 **	D > M P > M	0.52	-
Calcified cartilage cleft	0.005 *	D > M P > M	1.0	-
Calcified cartilage depth variation	<0.001 **	D > M P > M	0.20	-
Vascular invasion	<0.001 **	D > M P > M P > D	0.003 *	M > P
Islands of hyaline cartilage in subchondral bone plate	<0.001 **	D > M D > P	0.04 *	M > P
Summary of calcified cartilage	<0.001 **	D > M P > M	0.06	-
Subchondral plate and trabecular bone				
Sclerosis of subchondral bone plate and adjacent cancellous bone	0.000 **	P > M P > D	<0.001 **	D > P M > P
Subchondral bone collapse	<0.001 **	P > M P > D	0.04 *	D > P
Replacement of cancellous bone with dense bone	<0.001 **	P > M P > D	<0.001 **	D > P M > P
Trabecular thickening with reduced marrow spaces	<0.001 **	D > M P > M	<0.001 **	D > P M > P
Replacement with osteonal/lamellar bone	<0.001 **	D > M P > M P > D	<0.001 **	D > P M > P
Increased basic multicellular units	<0.001 **	P > M P > D	<0.001 **	D > P M > P
Replacement with woven bone	<0.001 **	P > M	0.42	-
Howship's lacunae with/without osteoclast	0.14		0.73	-
Summary of subchondral plate and trabecular bone	<0.001 **	P > M P > D	<0.001 **	D > P M > P

* Significant difference (fissure > non-fissure). ** Highly significant difference (fissure > non-fissure).

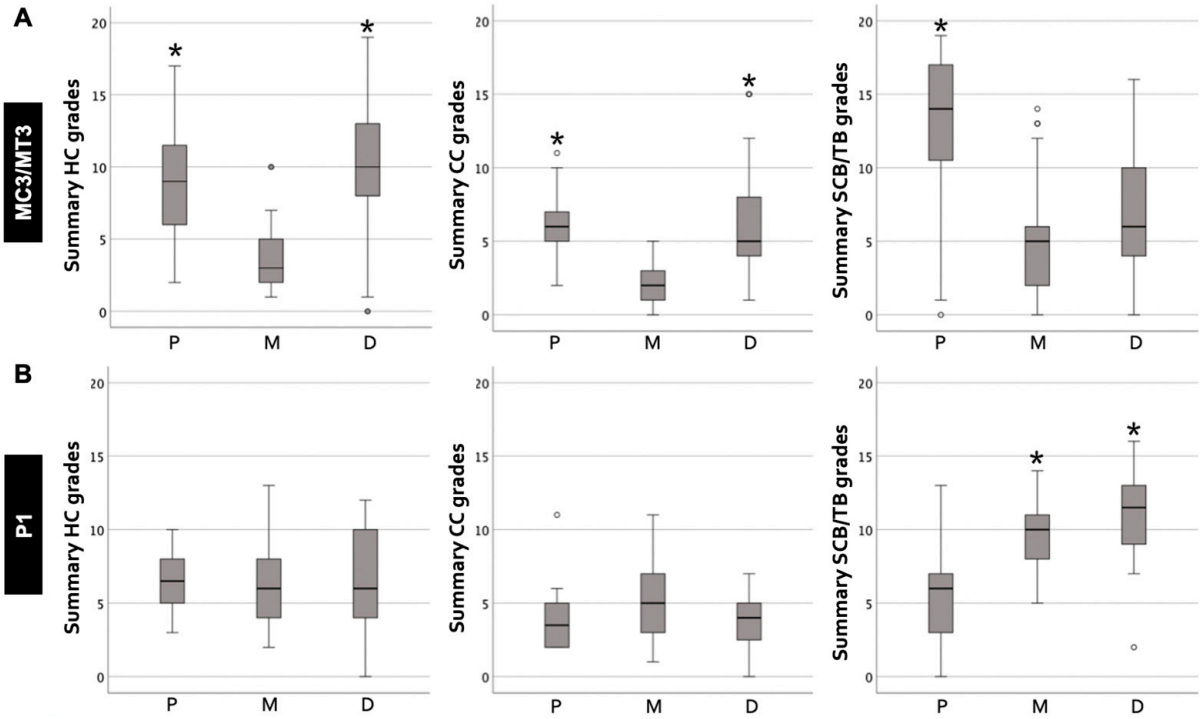


Figure 6. Summary of histological grades compared between dorsal, middle, and palmar/plantar aspects. HC (hyaline cartilage); CC (calcified cartilage); SCB/TB (subchondral plate and trabecular bone). (**A**) HC, CC, and SCB/TB histological grades were more severe in the palmar/plantar (P) aspect, and the HC and CC histological grades were more severe in the dorsal (D) aspect than the middle aspect (M) in the third metacarpal/tarsal parasagittal groove (MC3/MT3). (**B**) SCB/TB histological grades were more severe in the D and M aspects than the P aspect in the proximal phalanx sagittal groove (P1). * Significant difference ($p < 0.001$). Circles above or below the end of the whiskers represented outliers.

3.2.1. MC3/MT3 Parasagittal Groove

The median value and interquartile range of the summary of histological grades for (1) the dorsal aspect were 10.0 ± 5.0 in the HC region ($n = 40$), 5.0 ± 4.0 in the CC region ($n = 39$), and 6.0 ± 7.0 in the SCB/TB region ($n = 41$); (2) for the middle aspect were 3.0 ± 3.0 in the HC region ($n = 48$), 2.0 ± 2.0 in the CC region ($n = 47$), and 5.0 ± 5.0 in the SCB/TB region ($n = 54$); and (3) for the palmar/plantar aspect were 9.0 ± 6.0 in the HC region ($n = 47$), 6.0 ± 2.0 in the CC region ($n = 46$), and 14.0 ± 7.0 in the SCB/TB region ($n = 56$). The summaries of the HC and CC histological grades were more severe in the dorsal and palmar/plantar than the middle aspects ($p < 0.001$), and the summary of the SCB/TB histological grades was more severe in the palmar/plantar than the dorsal and middle aspects ($p < 0.001$) (Figure 3).

3.2.2. P1 Sagittal Groove

The median value and interquartile range of the summary of histological grades for (1) the dorsal aspect were 6.0 ± 6.0 in the HC region ($n = 24$), 4.0 ± 3.0 in the CC region ($n = 23$), and 11.5 ± 4.0 in the SCB/TB region ($n = 26$); (2) for the middle aspect were 6.0 ± 4.0 in the HC region ($n = 25$), 5.0 ± 5.0 in the CC region ($n = 25$), and 10.0 ± 3.0 in the SCB/TB region ($n = 27$); and (3) for the palmar/plantar aspect were 6.5 ± 3.0 in the HC region ($n = 22$), 3.5 ± 3.0 in the CC region ($n = 22$), and 6.0 ± 5.0 in the SCB/TB region ($n = 25$). The summary of the SCB/TB histological grades was more severe in the dorsal and middle than the palmar/plantar aspects ($p < 0.001$), while there was no significant difference in the summaries of the HC and CC histological grades (Figure 3).

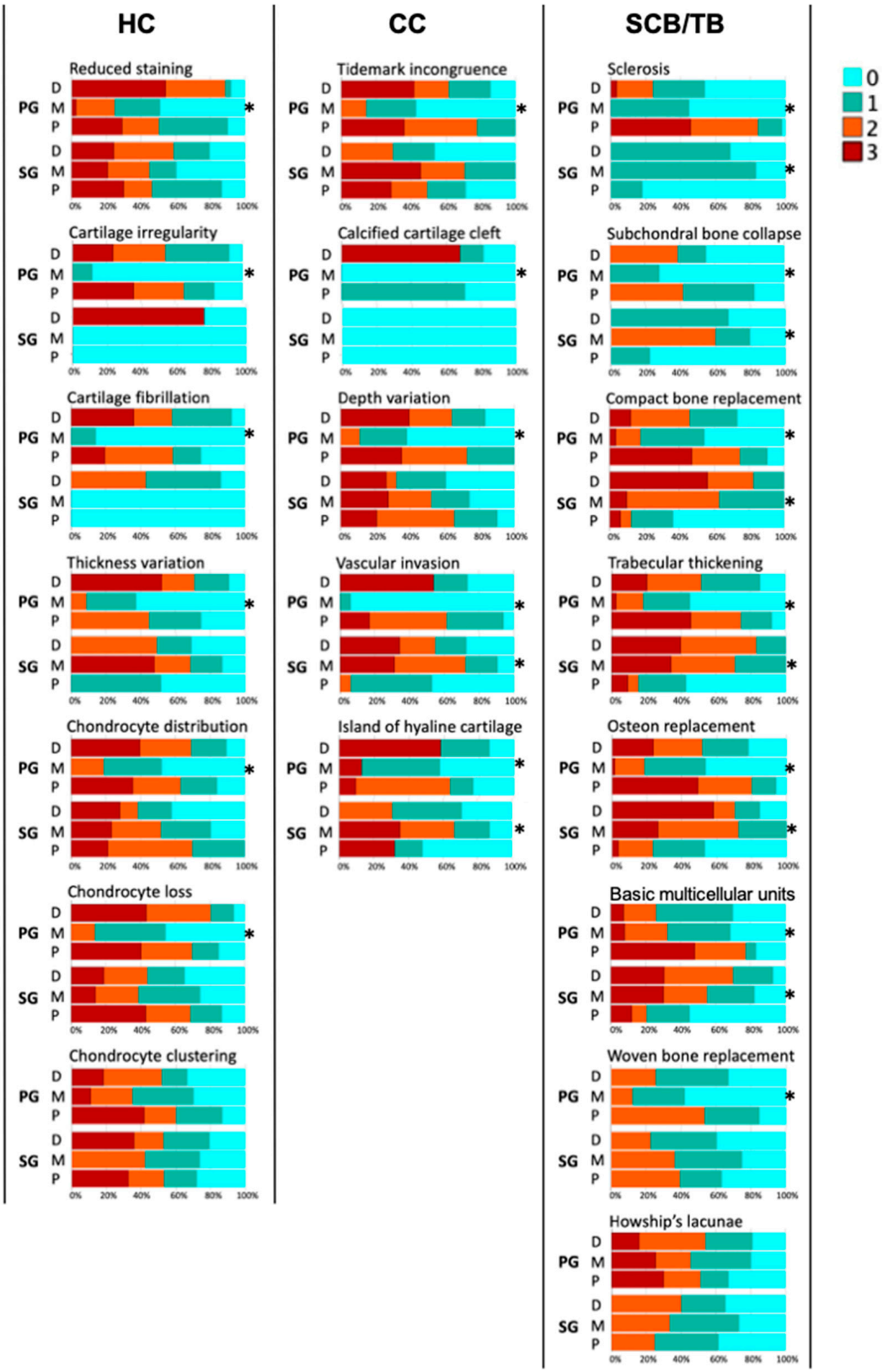


Figure 7. Proportion of grades for dorsal, middle, and palmar/plantar aspects. HC (hyaline cartilage); CC (calcified cartilage); SCB/TB (subchondral plate and trabecular bone); PG (third metacarpal/metatarsal parasagittal groove); SG (proximal phalanx sagittal groove); D (dorsal); M (middle); P (palmar/plantar). * Significant difference ($p < 0.05$).

4. Discussion

This study compared and described histopathological features of the MC3/MT3 parasagittal groove and P1 sagittal groove. The results of different histopathological features observed in the hyaline cartilage (HC) and calcified cartilage (CC) regions do not support our first hypothesis, that histopathological features of locations with fissures would be similar between the MC3/MT3 parasagittal groove and P1 sagittal groove. The severe histopathological changes in predilection sites of parasagittal fractures and sagittal fractures, including the palmar/plantar aspect of the MC3/MT3 parasagittal groove and the dorsal and middle aspects of the P1 sagittal groove, do support our second hypothesis that the predilection sites would be more associated with histopathological features related to fatigue injuries.

Fissure locations in the MC3/MT3 parasagittal groove were related to (1) SCB/TB changes indicating subchondral bone functional adaptation (e.g., sclerosis), bone fatigue injury (e.g., subchondral bone collapse), and initial bone repair (e.g., woven bone replacement) [8,11,15,27–31]; (2) CC changes indicating endochondral ossifications and functional adaptation (e.g., tidemark incongruence and vascular invasion) [8,32,33]; and (3) HC changes indicating matrix remodelling and tissue strain from strenuous exercise (e.g., reduced staining and irregular chondrocyte distribution) [15,34]. Similar SCB/TB, CC, and HC histopathological changes were also reported in fissure locations at the palmar/plantar aspect of the MC3/MT3 parasagittal groove in Thoroughbred racehorses [8,11,15].

Histopathological features in the palmar/plantar aspect of the MC3/MT3 parasagittal groove identified in this study corresponded to previous studies [8,11,15]. SCB/TB, CC, and HC changes were more severe in the palmar/plantar than the middle aspect. However, there was no difference in the severity of CC and HC changes between the palmar/plantar and dorsal aspects. Considering that the dorsal aspect of the MC3/MT3 bone is commonly affected by traumatic impact during fetlock joint hyperextension, the severe CC and HC changes in the dorsal parasagittal groove could reflect osteoarthritic changes [35–37]. In contrast, the severe SCB/TB changes in the palmar/plantar parasagittal groove indicated a stronger relationship with subchondral bone functional adaptation and fatigue injuries.

The histopathological features of fissure locations in the P1 sagittal groove were clearly different from the MC3/MT3 parasagittal groove in this study, particularly in the HC and CC regions. The finding that there was no HC histopathology associated with fissure locations may explain the previously reported lack of observation of pre-existing articular cartilage damage in proximal phalanx sagittal groove fractures as subchondral bone pathology could be hidden underneath the normal articular cartilage [38]. Vascular invasion was the only CC change associated with fissure locations and was known to represent endochondral ossifications in the progression of osteoarthritis [8,32,33]. In contrast to the HC and CC regions, SCB/TB changes indicating subchondral bone functional adaptation and bone fatigue injury were related to fissure locations in the P1 sagittal groove [8,11,15,27], which were similar to findings in the MC3/MT3 parasagittal groove. Considering the small number of non-fissure locations available for comparison in this study, care must be taken not to over-interpret the results of comparison.

SCB/TB changes in the dorsal and middle aspects of the P1 sagittal groove indicated subchondral bone functional adaptation, corresponding to the previously reported finding of increased subchondral bone thickness at the dorsal and middle aspects of the P1 sagittal groove in racehorses [25]. Furthermore, histopathological indications of fatigue injuries were also seen in the dorsal P1 sagittal, corresponding to the imaging finding that the dorsal aspect of the P1 sagittal groove is the most common predilection site of sagittal fractures [20,39].

In both the MC3/MT3 parasagittal groove and P1 sagittal groove, there are concurrent findings of vascular invasion in the CC region and increased BMU and subchondral bone collapse in the SCB/TB region. These findings correspond to the scenario proposed in the previous studies that bone remodelling (e.g., osteoclast activation and bone resorption in response to microdamage) were related to cross-talk between subchondral bone

and articular cartilage at the osteochondral junction (e.g., angiogenesis), and once the microdamage accumulates and exceeds the capacity of self-repairing, bone failure (e.g., subchondral bone collapse) and fatigue fracture could occur [32,33,40–44]. The result that these histopathologies were all associated with fissures and predilection sites of stress fractures in both MC3/MT3 and P1 in this study could add further support to the theory of bone maladaptation.

The different histopathological features observed between the MC3/MT3 parasagittal groove and P1 sagittal groove, particularly in the HC and CC regions, might be related to the difference in pressure distribution during loading [45,46]. It was reported that the biomechanical properties of articular cartilage such as glycosaminoglycan content and collagen level varied depending on the consistency of loading and range of shear strain [45]. It was also found that different from the middle aspect of distal MC3, which was subjected to both compressive and shear strains, the middle aspect of proximal P1 was mainly subjected to shear strains [46]. The components of articular cartilage were not analysed in this study; further investigation may be needed to clarify the effect of biomechanics on cartilage histopathology in MC3/MT3 and P1.

In the P1 sagittal groove, the SCB/TB histopathological findings from our study indicated that subchondral and trabecular bone sclerosis, bone remodelling, and failure of functional adaptation of bone were associated with both fissure locations and predilection sites of P1 sagittal groove fracture. These findings support clinical experience of bone failure at this location in horses undertaking high-intensity training and the previous suggestion that pathology may be related to repetitive loading [17,18,21,25,47]. These results support previous descriptions of clinical patients reporting marked subchondral bone thickening on radiographic images and increased fluid signal around the P1 sagittal groove on magnetic resonance imaging as potential prodromal diagnostic imaging features of increased risk of bone failure at this location [17–20,48]. The findings from our study may therefore be useful to add weight to the value of imaging in decision-making for these type of cases [17,20,48].

Limitations of this study included the small number of cadaver limbs from a small number of horses. Also, multiple bone specimens collected from individual limbs (a maximum number of nine specimens from a limb) and horses could result in clustering, and the histopathological features may not be representative for the entire Thoroughbred population. However, the newly reported histopathological findings in the P1 sagittal groove in Thoroughbred racehorses provided valuable information that has been lacking and may be useful as a comparison for future investigation on the pathogenesis of P1 sagittal groove fractures or fissures. Also, the histopathological findings in the MC3/MT3 parasagittal groove corresponded to previous histopathological studies, strengthening the association between the palmar/plantar MC3/MT3 parasagittal groove fissures and the failure of subchondral bone functional adaptation. Data from forelimbs and hindlimbs, right and left forelimbs, and medial and lateral parasagittal grooves were pooled together and were not analysed separately to avoid leaving a small number or even no samples remaining in a stratified group. However, the authors were aware that condylar and P1 fractures occur most commonly in forelimbs and lateral parasagittal grooves, and active osseous pathology in the P1 sagittal groove was more common in hindlimbs than forelimbs [1–3,12,49,50]. The small number of non-fissure locations in the P1 sagittal groove limited the interpretation of the histopathological features of fissure locations. However, histopathological findings at the dorsal and middle aspects of the P1 sagittal groove may partly support the relationship between the predilection site of P1 sagittal groove fracture and the failure of subchondral bone functional adaptation. Although histopathological changes indicating bone fatigue such as subchondral bone collapse were assessed in this study, microdamage was not assessable due to the lack of basic fuchsin staining. As an alternative, the increased occurrence of BMU was assessed based on previous studies reporting the concurrent finding of BMU with microdamage, but the limitation that BMU can also represent normal bone remodelling is fully appreciated [51–53]. The histological grading in this study was conducted by a single observer, and the data would be more

robust if two individual gradings could be established. Finally, the study only included Thoroughbred horses that had been in racing or race-training, and not all cadaver limbs had clinically relevant lameness or disease. A future study with control Thoroughbred horses and cadaver limbs is needed to validate the physiological and/or pathological background of the histopathological changes identified in this study.

5. Conclusions

In conclusion, fissures in the MC3/MT3 parasagittal groove and P1 sagittal groove could have similar pathogenesis to bone fatigue injuries, albeit with some differences at the cartilage level. Predilection sites of MC3/MT3 parasagittal fracture and P1 sagittal fracture had histopathology consistent with the failure of subchondral bone adaptation being involved in the pathogenesis.

Supplementary Materials: The following supporting information can be downloaded at: https://www.mdpi.com/article/10.3390/ani14131942/s1, Figure S1: Hyaline Cartilage; Figure S2: Calcified Cartilage; Figure S3: Subchondral bone plate and trabecular bone.

Author Contributions: Conceptualisation and methodology, S.-T.L., R.C.M., N.M.B., D.R.S., and A.K.F.; validation of pathology, A.K.F.; formal Analysis, S.-T.L.; investigation, S.-T.L., R.C.M. and N.M.B.; resources, R.C.M. and D.R.S.; writing—original draft preparation, S.-T.L.; writing—review and editing, R.C.M.; supervision, R.C.M., N.M.B. and D.R.S.; project administration, R.C.M. and D.R.S.; funding acquisition, R.C.M. and D.R.S. All authors have read and agreed to the published version of the manuscript.

Funding: This work was supported by Robinson College (Friends of the College Fund), the School of Biological Science (Charles Slater Fund 2021), and the Department of Veterinary Medicine, University of Cambridge and the Horserace Betting Levy Board (SPrj53). The funding sources had no involvement in the study design, collection, analysis and interpretation of data, the writing of the report, and the decision to submit the article for publication.

Institutional Review Board Statement: Approved by the University of Cambridge Ethical Review committee (project number: CR558).

Informed Consent Statement: Informed consent was obtained for all cadaver limbs included in the study using a signed consent form for each horse.

Data Availability Statement: The data that support the findings of this study are available on request from the corresponding author.

Acknowledgments: The authors thank Rossdales Laboratories for providing the pathological examination support for the study. We are very grateful to Sarah Bradfield and Michelle Haynes from Rossdales Laboratories for kindly providing histological preparation support. The authors thank Olivier Restif of the Department of Veterinary Medicine, University of Cambridge for providing the statistical analysis support. The study was funded by Robinson College, the Charles Slater Fund of the School of Biological Science, and the Department of Veterinary Medicine, University of Cambridge and the Horserace Betting Levy Board, to whom we are most grateful.

Conflicts of Interest: N. Bolas is employed by Hallmarq Veterinary Imaging.

References

1. Parkin, T.; French, N.; Riggs, C.; Morgan, K.; Clegg, P.; Proudman, C.; Singer, E.; Webbon, P. Risk of fatal distal limb fractures among thoroughbreds involved in the five types of racing in the United Kingdom. *Vet. Rec.* **2004**, *154*, 493–497. [CrossRef] [PubMed]
2. Parkin, T.D. Epidemiology of racetrack injuries in racehorses. *Vet. Clin. N. Am. Equine Pract.* **2008**, *24*, 1–19. [CrossRef] [PubMed]
3. Ramzan, P.H.; Palmer, L. Musculoskeletal injuries in Thoroughbred racehorses: A study of three large training yards in Newmarket, UK (2005–2007). *Vet. J.* **2011**, *187*, 325–329. [CrossRef] [PubMed]
4. Johnson, B.; Stover, S.M.; Daft, B.M.; Kinde, H.; Read, D.; Barr, B.; Anderson, M.; Moore, J.; Woods, L.; Stoltz, J. Causes of death in racehorses over a 2 year period. *Equine Vet. J.* **1994**, *26*, 327–330. [CrossRef] [PubMed]
5. Parkin, T.; Clegg, P.; French, N.; Proudman, C.; Riggs, C.; Singer, E.; Webbon, P.; Morgan, K. Horse-level risk factors for fatal distal limb fracture in racing Thoroughbreds in the UK. *Equine Vet. J.* **2004**, *36*, 513–519. [CrossRef] [PubMed]

6. Riggs, C.; Boyde, A. Effect of exercise on bone density in distal regions of the equine third metacarpal bone in 2-year-old Thoroughbreds. *Equine Vet. J.* **1999**, *31*, 555–560. [CrossRef] [PubMed]
7. Liley, H.; Davies, H.; Firth, E.; Besier, T.; Fernandez, J. The effect of the sagittal ridge angle on cartilage stress in the equine metacarpo-phalangeal (fetlock) joint. *Comput. Methods Biomech. Biomed. Eng.* **2017**, *20*, 1140–1149. [CrossRef] [PubMed]
8. Muir, P.; McCarthy, J.; Radtke, C.; Markel, M.; Santschi, E.M.; Scollay, M.; Kalscheur, V. Role of endochondral ossification of articular cartilage and functional adaptation of the subchondral plate in the development of fatigue microcracking of joints. *Bone* **2006**, *38*, 342–349. [CrossRef] [PubMed]
9. Riggs, C. Osteochondral injury and joint disease in the athletic horse. *Equine Vet. Educ.* **2006**, *18*, 100–112. [CrossRef]
10. Riggs, C.; Whitehouse, G.; Boyde, A. Pathology of the distal condyles of the third metacarpal and third metatarsal bones of the horse. *Equine Vet. J.* **1999**, *31*, 140–148. [CrossRef]
11. Muir, P.; Peterson, A.; Sample, S.; Scollay, M.; Markel, M.; Kalscheur, V. Exercise-induced metacarpophalangeal joint adaptation in the Thoroughbred racehorse. *J. Anat.* **2008**, *213*, 706–717. [CrossRef] [PubMed]
12. Parkin, T.; Clegg, P.; French, N.; Proudman, C.; Riggs, C.; Singer, E.; Webbon, P.; Morgan, K. Catastrophic fracture of the lateral condyle of the third metacarpus/metatarsus in UK racehorses–fracture descriptions and pre-existing pathology. *Vet. J.* **2006**, *171*, 157–165. [CrossRef] [PubMed]
13. Radtke, C.L.; Danova, N.A.; Scollay, M.C.; Santschi, E.M.; Markel, M.D.; Gómez, T.D.C.; Muir, P. Macroscopic changes in the distal ends of the third metacarpal and metatarsal bones of Thoroughbred racehorses with condylar fractures. *Am. J. Vet. Res.* **2003**, *64*, 1110–1116. [CrossRef] [PubMed]
14. Johnston, G.C.; Ahern, B.J.; Palmieri, C.; Young, A.C. Imaging and gross pathological appearance of changes in the parasagittal grooves of Thoroughbred racehorses. *Animals* **2021**, *11*, 3366. [CrossRef] [PubMed]
15. Turley, S.M.; Thambyah, A.; Riggs, C.M.; Firth, E.C.; Broom, N.D. Microstructural changes in cartilage and bone related to repetitive overloading in an equine athlete model. *J. Anat.* **2014**, *224*, 647–658. [CrossRef] [PubMed]
16. Dubois, M.-S.; Morello, S.; Rayment, K.; Markel, M.D.; Vanderby, R., Jr.; Kalscheur, V.L.; Hao, Z.; McCabe, R.P.; Marquis, P.; Muir, P. Computed tomographic imaging of subchondral fatigue cracks in the distal end of the third metacarpal bone in the thoroughbred racehorse can predict crack micromotion in an ex-vivo model. *PLoS ONE* **2014**, *9*, e101230. [CrossRef] [PubMed]
17. Ramzan, P.; Powell, S. Clinical and imaging features of suspected prodromal fracture of the proximal phalanx in three Thoroughbred racehorses. *Equine Vet. J.* **2010**, *42*, 164–169. [CrossRef] [PubMed]
18. Smith, M.; Wright, I. Are there radiologically identifiable prodromal changes in T horoughbred racehorses with parasagittal fractures of the proximal phalanx? *Equine Vet. J.* **2014**, *46*, 88–91. [CrossRef] [PubMed]
19. Kuemmerle, J.M.; Auer, J.A.; Rademacher, N.; Lischer, C.J.; Bettschart-Wolfensberger, R.; Fürst, A.E. Short incomplete sagittal fractures of the proximal phalanx in ten horses not used for racing. *Vet. Surg.* **2008**, *37*, 193–200. [CrossRef]
20. Dyson, S.; Nagy, A.; Murray, R. Clinical and diagnostic imaging findings in horses with subchondral bone trauma of the sagittal groove of the proximal phalanx. *Vet. Radiol. Ultrasound* **2011**, *52*, 596–604. [CrossRef]
21. Gold, S.J.; Werpy, N.M.; Gutierrez-Nibeyro, S.D. Injuries of the sagittal groove of the proximal phalanx in warmblood horses detected with low-field magnetic resonance imaging: 19 cases (2007–2016). *Vet. Radiol. Ultrasound* **2017**, *58*, 344–353. [CrossRef]
22. Ammann, L.; Fürst, A.E.; Jackson, M.A. Complete fractures through osseous cyst-like lesions of the proximal phalanx in three horses. *Equine Vet. Educ.* **2024**. [CrossRef]
23. Ammann, L.; Ohlerth, S.; Fürst, A.E.; Jackson, M.A. Differences of morphological attributes between 62 proximal and distal subchondral cystic lesions of the proximal phalanx as determined by radiography and computed tomography. *Am. J. Vet. Res.* **2022**, *83*, ajvr.22.04.0071. [CrossRef] [PubMed]
24. Faulkner, J.E.; Joostens, Z.; Broeckx, B.J.; Hauspie, S.; Mariën, T.; Vanderperren, K. Follow-Up Magnetic Resonance Imaging of Sagittal Groove Disease of the Equine Proximal Phalanx Using a Classification System in 29 Non-Racing Sports Horses. *Animals* **2023**, *14*, 34. [CrossRef]
25. Noble, P.; Singer, E.R.; Jeffery, N.S. Does subchondral bone of the equine proximal phalanx adapt to race training? *J. Anat.* **2016**, *229*, 104–113. [CrossRef] [PubMed]
26. Lin, S.-T.; Foote, A.K.; Bolas, N.M.; Peter, V.G.; Pokora, R.; Patrick, H.; Sargan, D.R.; Murray, R.C. Three-Dimensional Imaging and Histopathological Features of Third Metacarpal/Tarsal Parasagittal Groove and Proximal Phalanx Sagittal Groove Fissures in Thoroughbred Horses. *Animals* **2023**, *13*, 2912. [CrossRef] [PubMed]
27. Pinilla, M.; Tranquille, C.; Blunden, A.; Chang, Y.; Parkin, T.; Murray, R. Histological features of the distal third metacarpal bone in thoroughbred racehorses, with and without lateral condylar fractures. *J. Comp. Pathol.* **2017**, *157*, 1–10. [CrossRef]
28. Shapiro, F.; Wu, J.Y. Woven bone overview: Structural classification based on its integral role in developmental, repair and pathological bone formation throughout vertebrate groups. *Eur. Cells Mater.* **2019**, *38*, 137–167. [CrossRef]
29. Sugiyama, T.; Meakin, L.B.; Browne, W.J.; Galea, G.L.; Price, J.S.; Lanyon, L.E. Bones' adaptive response to mechanical loading is essentially linear between the low strains associated with disuse and the high strains associated with the lamellar/woven bone transition. *J. Bone Miner. Res.* **2012**, *27*, 1784–1793. [CrossRef]
30. Herman, B.C.; Cardoso, L.; Majeska, R.J.; Jepsen, K.J.; Schaffler, M.B. Activation of bone remodeling after fatigue: Differential response to linear microcracks and diffuse damage. *Bone* **2010**, *47*, 766–772. [CrossRef]
31. Whitton, R.; Ayodele, B.; Hitchens, P.; Mackie, E. Subchondral bone microdamage accumulation in distal metacarpus of Thoroughbred racehorses. *Equine Vet. J.* **2018**, *50*, 766–773. [CrossRef]

32. Mapp, P.I.; Walsh, D.A. Mechanisms and targets of angiogenesis and nerve growth in osteoarthritis. *Nat. Rev. Rheumatol.* **2012**, *8*, 390–398. [CrossRef]
33. Donell, S. Subchondral bone remodelling in osteoarthritis. *EFORT Open Rev.* **2019**, *4*, 221. [CrossRef] [PubMed]
34. Murray, R.; Zhu, C.; Goodship, A.; Lakhani, K.; Agrawal, C.; Athanasiou, K. Exercise affects the mechanical properties and histological appearance of equine articular cartilage. *J. Orthop. Res.* **1999**, *17*, 725–731. [CrossRef]
35. Santschi, E.M. Articular fetlock injuries in exercising horses. *Vet. Clin. N. Am. Equine Pract.* **2008**, *24*, 117–132. [CrossRef]
36. Bramlage, L.R. Part I: Operative orthopedics of the fetlock joint of the horse: Traumatic and developmental diseases of the equine fetlock joint. *Proc. Am. Ass. Equine Pr.* **2009**, *55*, 96–143.
37. Vanderperren, K.; Saunders, J.H. Diagnostic imaging of the equine fetlock region using radiography and ultrasonography. Part 1: Soft tissues. *Vet. J.* **2009**, *181*, 111–122. [CrossRef] [PubMed]
38. Richardson, D.W. Fractures of the proximal phalanx. *Equine Fract. Repair* **2019**, *53*, 295–319.
39. Shepherd, M.; Meehan, J. The European Thoroughbred. *Equine Scintigr.* **2003**, *117*, 150.
40. Suri, S.; Walsh, D.A. Osteochondral alterations in osteoarthritis. *Bone* **2012**, *51*, 204–211. [CrossRef]
41. Kenkre, J.; Bassett, J. The bone remodelling cycle. *Ann. Clin. Biochem.* **2018**, *55*, 308–327. [CrossRef] [PubMed]
42. Hauge, E.M.; Qvesel, D.; Eriksen, E.F.; Mosekilde, L.; Melsen, F. Cancellous bone remodeling occurs in specialized compartments lined by cells expressing osteoblastic markers. *J. Bone Miner. Res.* **2001**, *16*, 1575–1582. [CrossRef] [PubMed]
43. Kawcak, C.E.; McIlwraith, C.W.; Norrdin, R.; Park, R.; James, S. The role of subchondral bone in joint disease: A review. *Equine Vet. J.* **2001**, *33*, 120–126. [CrossRef] [PubMed]
44. Seref-Ferlengez, Z.; Kennedy, O.D.; Schaffler, M.B. Bone microdamage, remodeling and bone fragility: How much damage is too much damage? *BoneKey Rep.* **2015**, *4*, 644. [CrossRef] [PubMed]
45. Brama, P.; Tekoppele, J.; Bank, R.; Karssenberg, D.; Barneveld, A.; Van Weeren, P. Topographical mapping of biochemical properties of articular cartilage in the equine fetlock joint. *Equine Vet. J.* **2000**, *32*, 19–26. [CrossRef] [PubMed]
46. Singer, E.; Garcia, T.; Stover, S. How does bone strain vary between the third metacarpal and the proximal phalangeal bones of the equine distal limb? *J. Biomech.* **2021**, *123*, 110455. [CrossRef] [PubMed]
47. Bailey, R.E.; Dyson, S.J.; Parkin, T.D. Focal increased radiopharmaceutical uptake in the dorsoproximal diaphyseal region of the equine proximal phalanx. *Vet. Radiol. Ultrasound* **2007**, *48*, 460–466. [CrossRef] [PubMed]
48. Lipreri, G.; Bladon, B.M.; Giorio, M.E.; Singer, E.R. Conservative versus surgical treatment of 21 sports horses with osseous trauma in the proximal phalangeal sagittal groove diagnosed by low-field MRI. *Vet. Surg.* **2018**, *47*, 908–915. [CrossRef] [PubMed]
49. Faulkner, J.E.; Joostens, Z.; Broeckx, B.J.; Hauspie, S.; Mariën, T.; Vanderperren, K. Low-field magnetic resonance imaging of sagittal groove disease of the proximal phalanx in non-racing sport horses. *Equine Vet. J.* **2024**. [CrossRef]
50. Bergstrom, T.C.; Spriet, M.; Carpenter, R.S.; Jacques, K.L.; Stover, S.M. Condylar fracture location is correlated to exercise history in Thoroughbred racehorses. *Equine Vet. J.* **2024**. [CrossRef]
51. Bertuglia, A.; Lacourt, M.; Girard, C.; Beauchamp, G.; Richard, H.; Laverty, S. Osteoclasts are recruited to the subchondral bone in naturally occurring post-traumatic equine carpal osteoarthritis and may contribute to cartilage degradation. *Osteoarthr. Cartil.* **2016**, *24*, 555–566. [CrossRef] [PubMed]
52. Ganghoffer, J.-F.; Rahouadj, R.; Boisse, J.; Forest, S. Phase field approaches of bone remodeling based on TIP. *J. Non-Equilib. Thermodyn.* **2016**, *41*, 49–75. [CrossRef]
53. Martin, R.; Gibson, V.; Stover, S.; Gibeling, J.; Griffin, L. In vitro fatigue behavior of the equine third metacarpus: Remodeling and microcrack damage analysis. *J. Orthop. Res.* **1996**, *14*, 794–801. [CrossRef] [PubMed]

Disclaimer/Publisher's Note: The statements, opinions and data contained in all publications are solely those of the individual author(s) and contributor(s) and not of MDPI and/or the editor(s). MDPI and/or the editor(s) disclaim responsibility for any injury to people or property resulting from any ideas, methods, instructions or products referred to in the content.